Chapter IV

Analysis of Scattered Waves from Burnt Coal Seam

4.1 Introduction

In 1995, the Indonesian Government released peat area (soil with about 40% to 60% coal content) in central Borneo to be converted into agricultural area. It was known as 'One Million Hectares Peatland Project' (Burhanuddin 2000, Tetuko 2001b). The project composed of four areas called Peatland Project (PLG) - A to D. This study chose PLG-A as the study area. The ground data of the study area were collected in the period 1995 to 1997 (figure 4.1, and detail in Appendix D). Figure 4.2 (a) shows the study area and its forestry landuse, then 4.2 (b) to (d) show distribution of coal seam thickness in the study area: 'One Million Hectares Peatland Project' District A (PLG-A), B (PLG-B) and D (PLG-D) at central Borneo, Indonesia (CSAR 1997). Figure 4.2 (b) to (d) are master plan of this project, where lines show irrigation canals (CSAR 1997). The study area in this study is PLG-A that is shown in figure 4.2 (b), where dotted lines show area of used Japanese Earth Resources Satellite (JERS-1) Synthetic Aperture Radar (SAR) data and Satellite Pour l'Observation de la Terre (SPOT) High Resolution Visible Imaging System (HRV) data that are used in this study. Construction of the canals was begun in April 1996 by Indonesian Department of Public Works. The colours in this map show the distribution of coal seam thickness.

In this project, vegetation was burnt to open up the area. These fire events caused coal seam fires that were difficult to extinguish, because fires penetrated to underground of peat that is known as flammable matter. Hence it was difficult to extinguish and to be detected by eyes (Hadi 1999, Kasdi 1999). It was important to investigate the thickness ξ of burnt coal

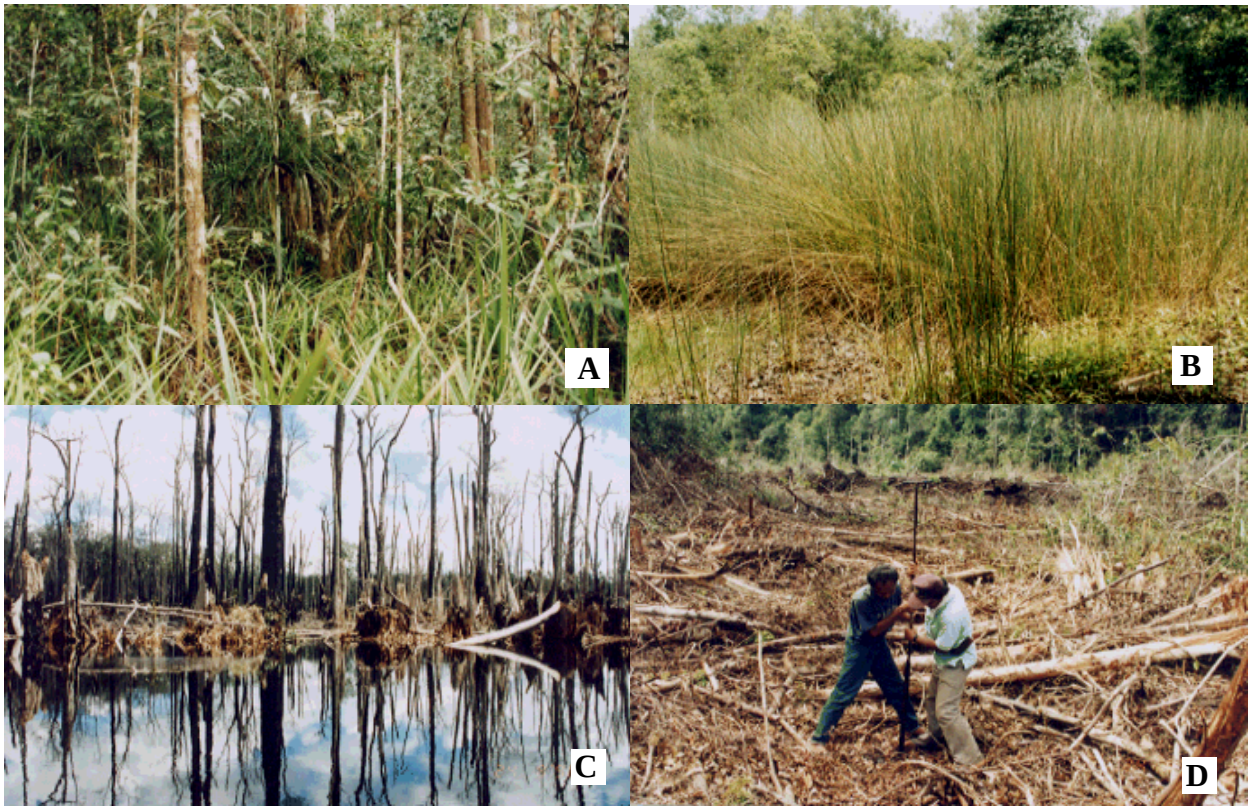

Figure 4.1. Photographs of field survey expeditions in period 1995 to 1997. A and B show main vegetations that found around study sites; Tengkawang (*Dipterocarpaceae spp.*) and *purun* grass, respectively. C shows burnt forest that remained burnt tree trunk and burnt coal seam. D shows staffs measured thickness of coal seam.

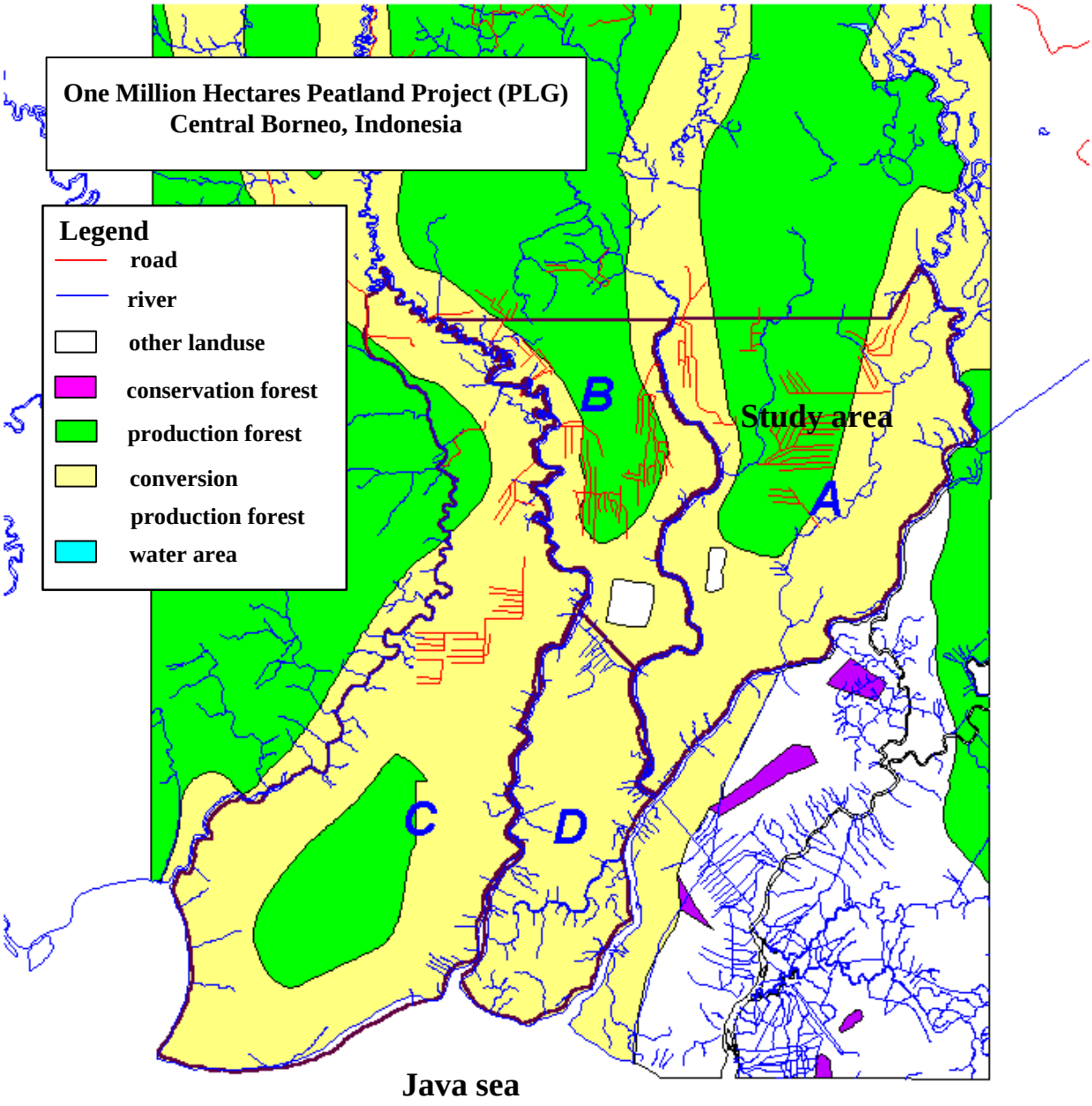

Figure 4.2 (a) Digital map of the study area: One Million Hectares Peatland Project (PLG), central Borneo, Indonesia (DEPHUTBUN 1999).

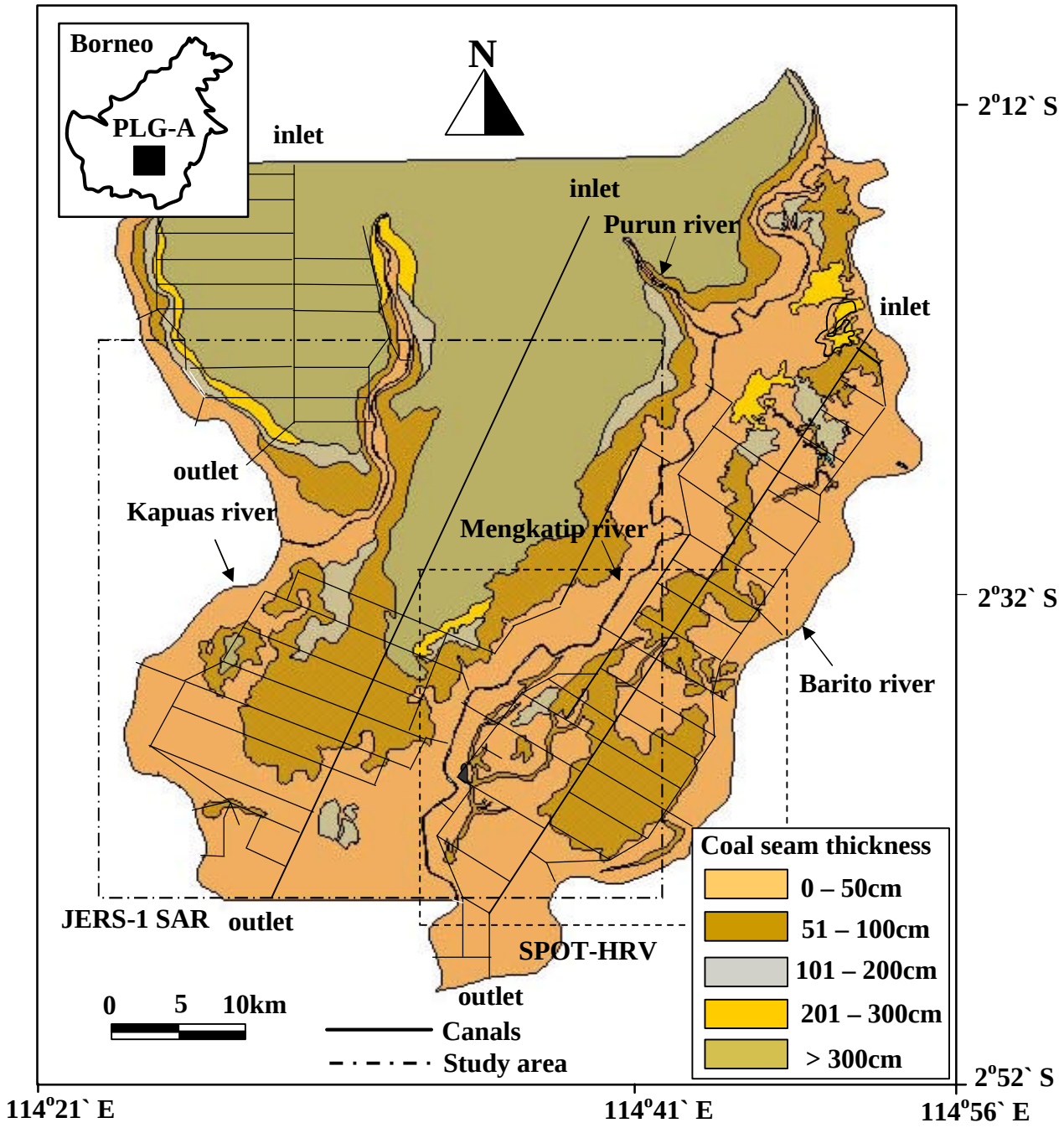

Figure 4.2 (b) Study area: master plan of 'One Million Hectares Peatland Project (PLG)' at central Borneo, Indonesia. This figure shows thickness of coal seam that collected in field survey expeditions in period 1995 to 1997. Dotted lines show the area covered by JERS-1 SAR and SPOT HRV data.

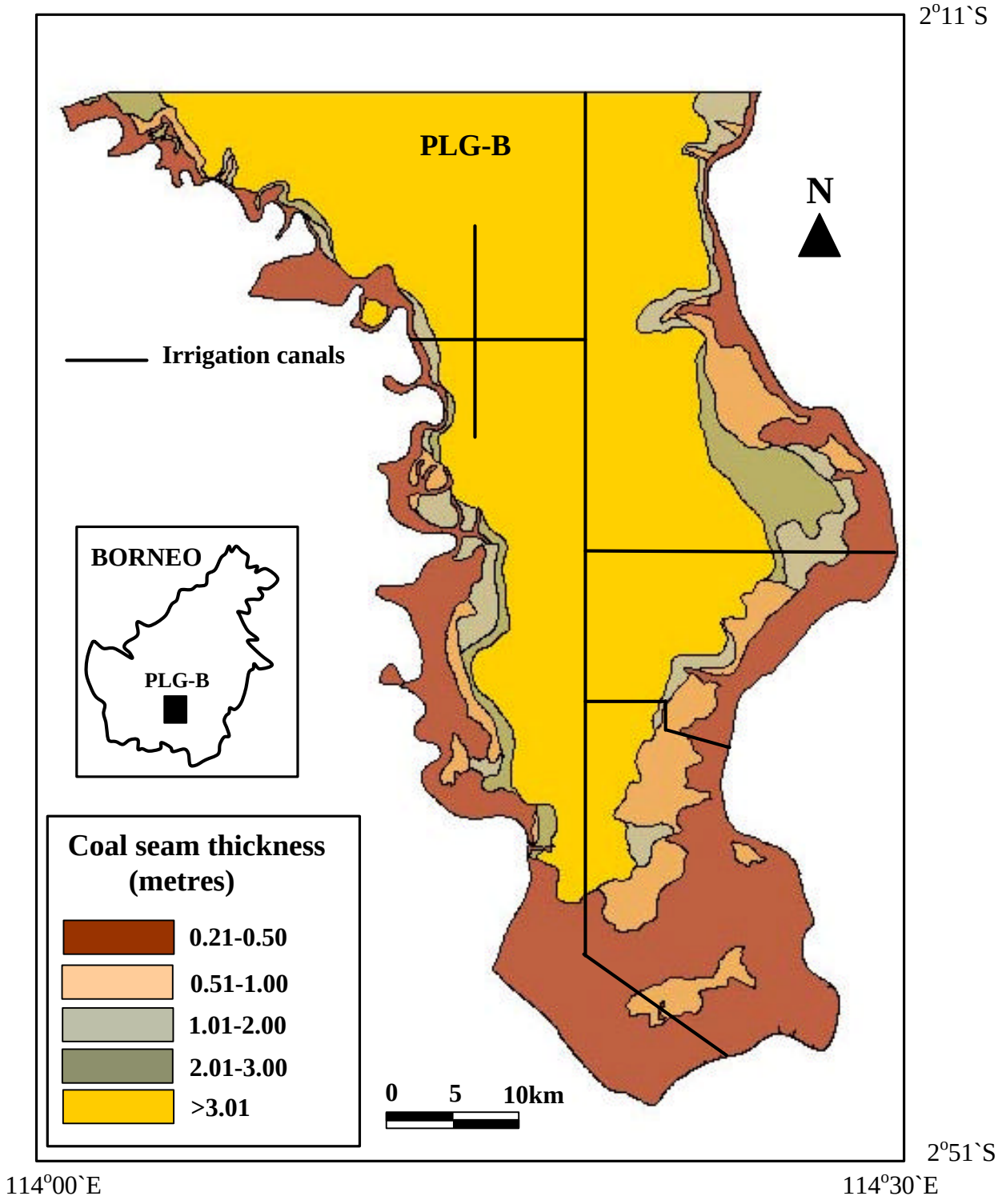

Figure 4.2 (c). Distribution of the thickness of coal seam: One Million Hectares Peatland Project, District B (PLG-B) at central Borneo, Indonesia

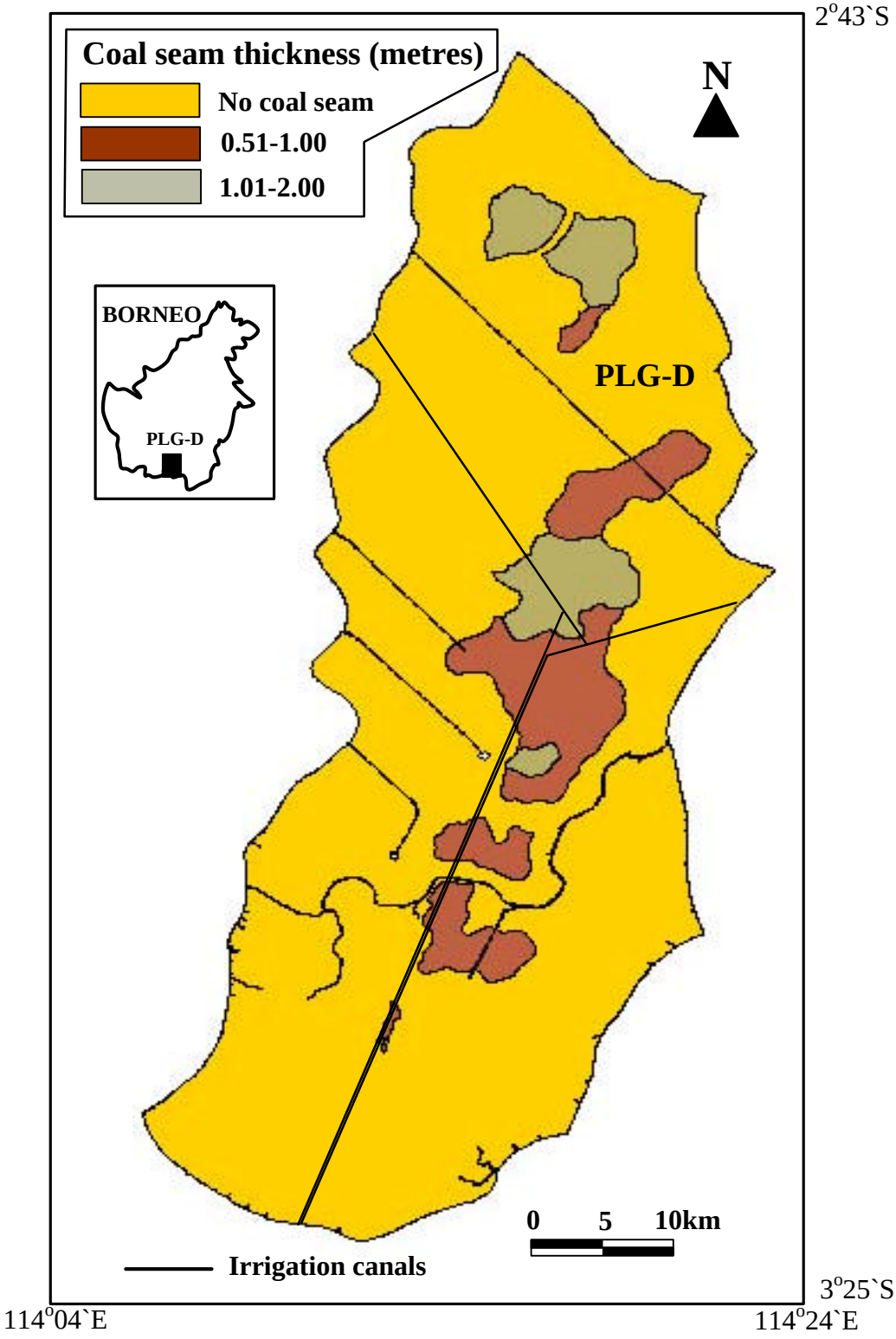

Figure 4.2 (d). Distribution of the thickness of coal seam: One Million Hectares Peatland Project, District D (PLG-D) at central Borneo, Indonesia

seam in order to protect the spreading of fire and to detect the fire spots in early stage and efficiently.

The effect of fires were inferred from SPOT HRV data acquired on 6 June 1997 (prior fire), 29 July 1997 and 7 August 1997 (during fire), and 8 September 1997 (after fire), see figure 4.3. Figure 4.3 (a) shows the construction of canals in PLG-A on 6 June 1997 that would be used for transportation and irrigation to planned agricultural area. Figure 4.3 (b) and 4.3 (c) show peat area under man-made fires on 29 July and 7 August 1997. Figure 4.3(d) shows the area after the fires occurred. This area will be used as agricultural area by Indonesian Department of Forestry and Estate Crops (Burhanuddin 2000). In this study, JERS-1 SAR data acquired on 29 July 1997, during the fires, is used to estimate the thickness ξ of burnt coal seam of the study area.

In this study, analysis and simulation of scattered waves from burnt coal seam are done in order to estimate the relationship between ξ and its backscattering coefficient s^{o}. In section 4.2, modelling of scattering problems in burnt coal seam and the formulation of it are reviewed using the classical or simple transmission line circuit method. In section 4.3, simulation of transverse electric (TE) wave propagation in burnt coal seam is conducted by Finite Difference Time Domain (FDTD) method (Tetuko *et al*. 2001a, Tetuko *et al.* 2001b, Uno 1998). The Mur method is applied as the absorbing boundary condition or the external condition to absorb the outgoing electromagnetic waves in simulation space edges. In section 4.4, analytical results are verified by comparing them with simulated ones. Application of these results is presented in section 4.5. In this section, the possibility of relationship between backscattering coefficient s^{0} and thickness ξ of burnt coal seam is used to estimate the thickness of the burnt coal seam ξ from JERS-1 SAR data is evaluated. Finally, the conclusions are given in section 4.6.

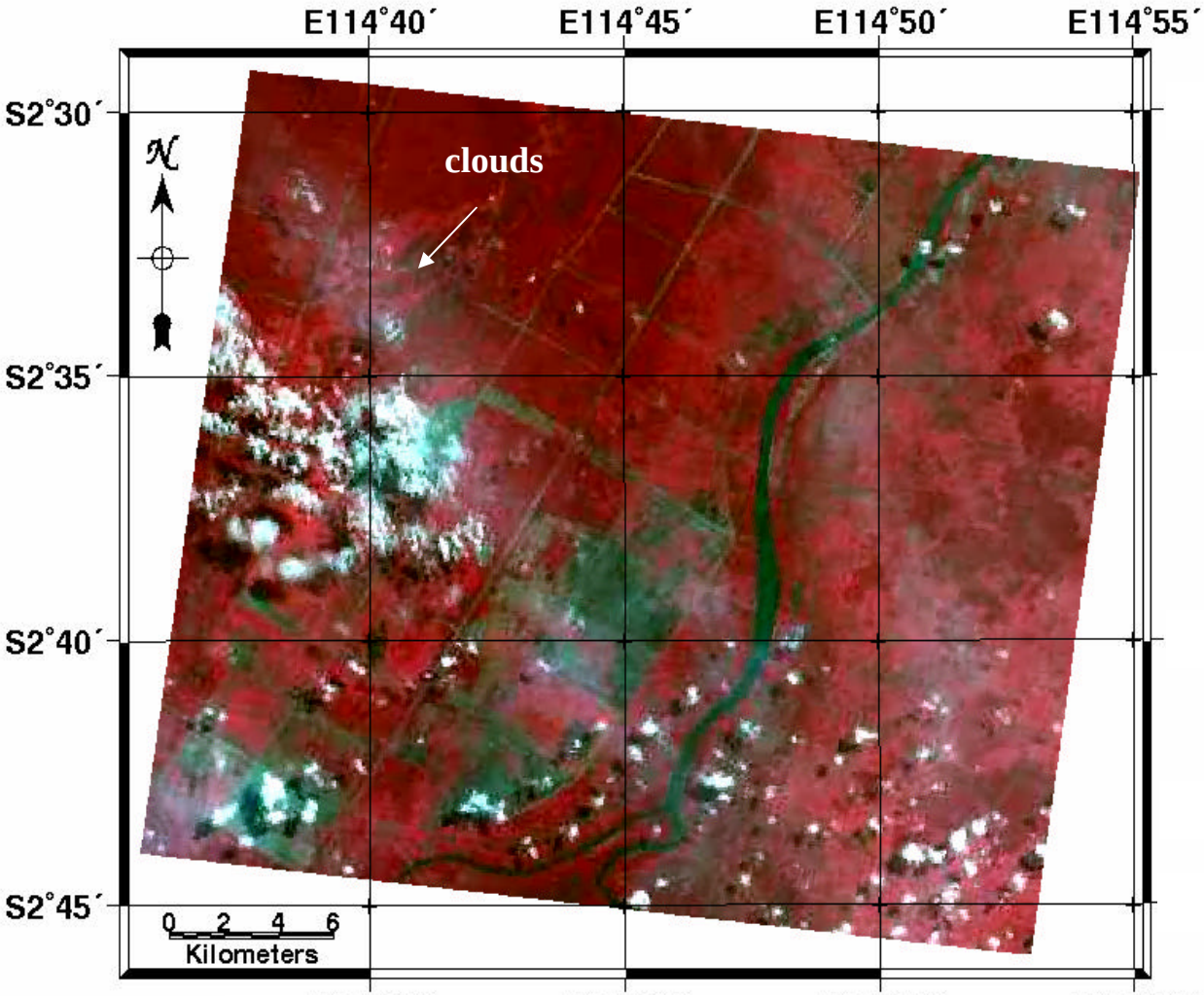

Figure 4.3 (a) SPOT HRV data of fire events in the study area, 6 June 1997 (prior to the fire).

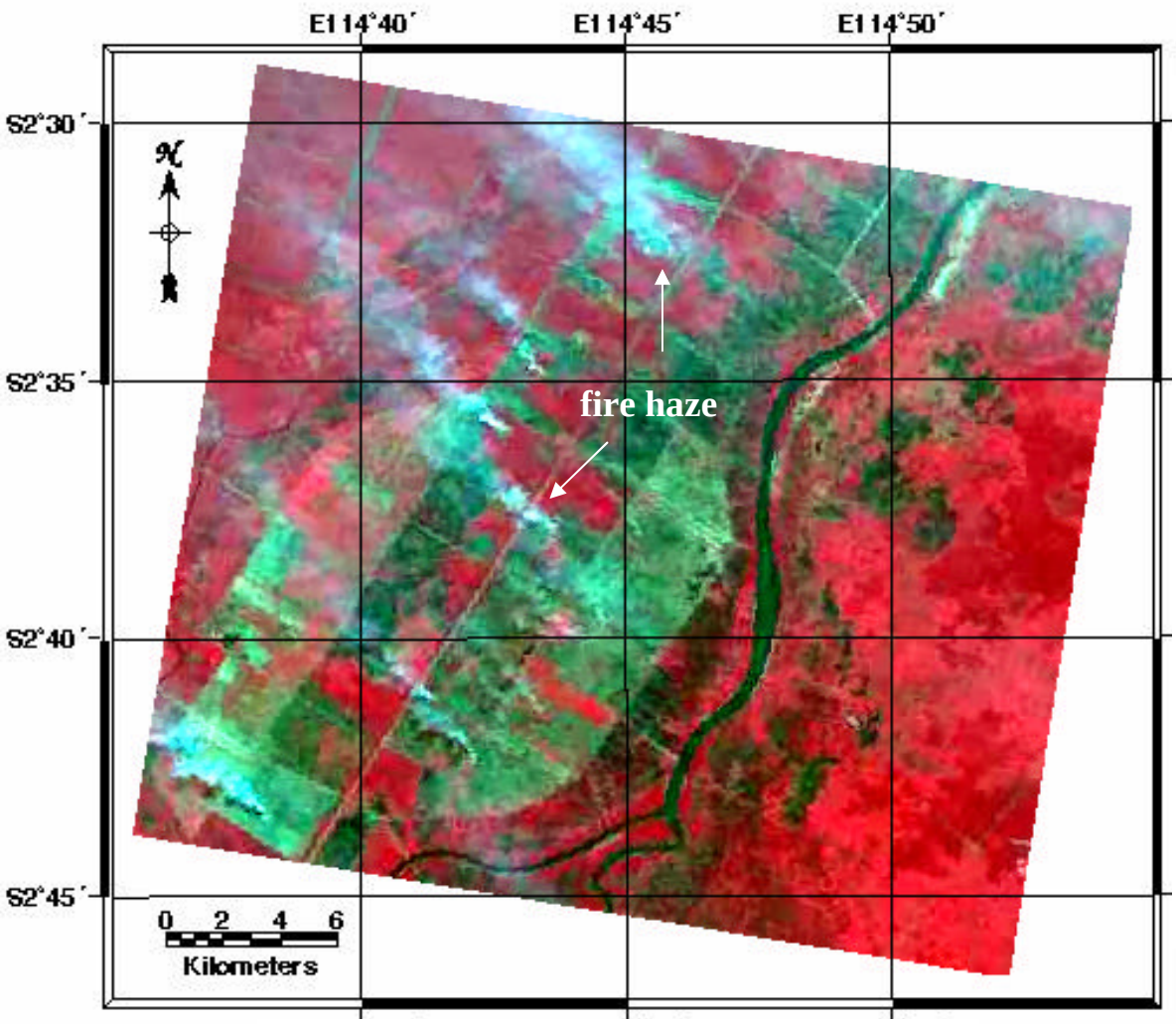

Figure 4.3 (b). SPOT HRV data of fire events in the study area, 29 July 1997 (during fire).

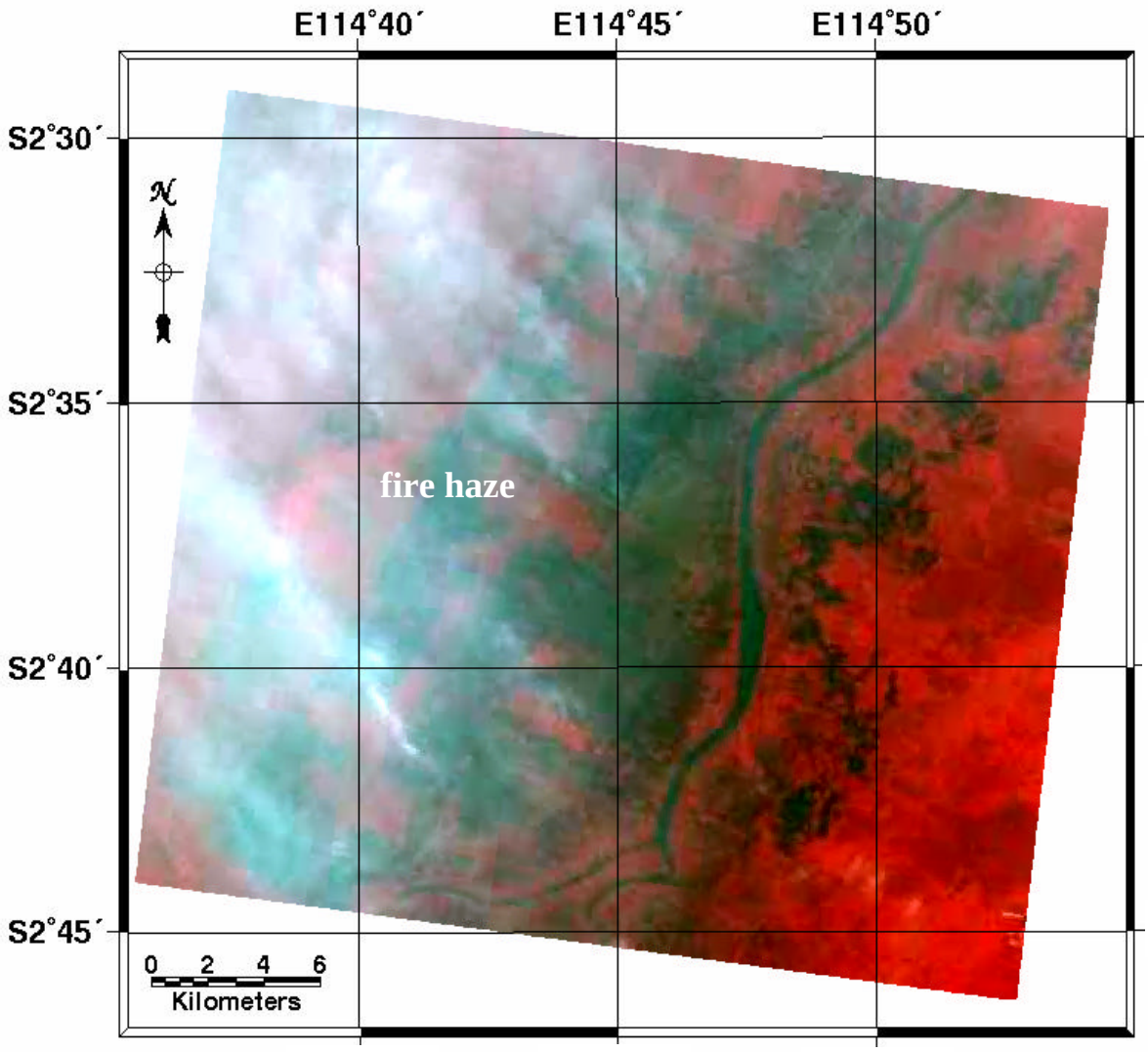

Figure 4.3 (c). SPOT HRV data of fire events in the study area, 7 August 1997 (during fire). .

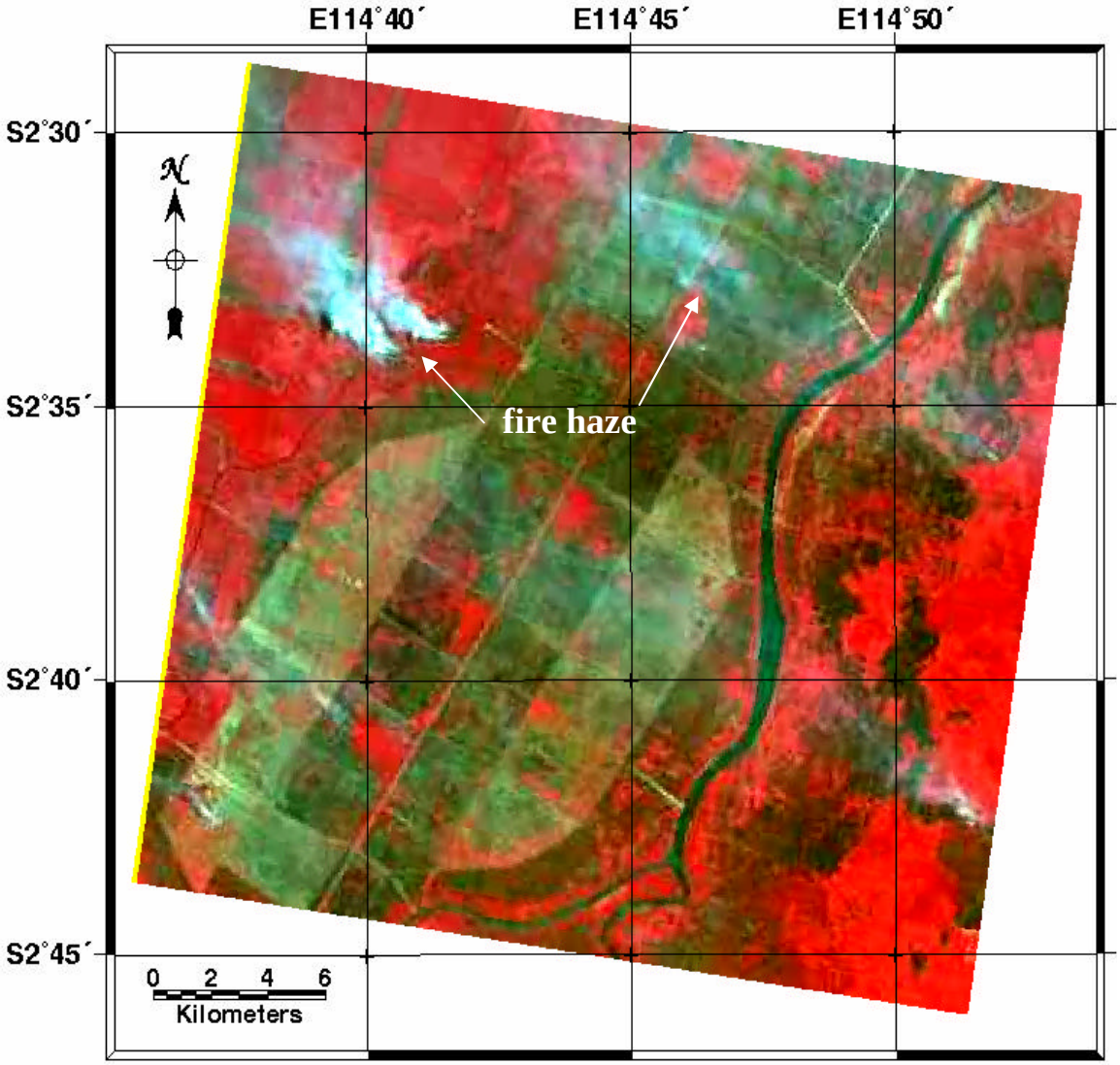

Figure 4.3 (d). SPOT HRV data of fire events in the study area, 8 September 1997 (after fire).

4.2 Analysis

Several field surveys were done in period of 1995 to 1997 to collect ground data. The ground data shows fire scars in central Borneo were covered by burnt coal seam that was produced by the burnt tropical forest or tree trunk and the burnt peat, see Figure 4.1(C) and Figure 4.1(D). In this study, the burnt coal seam is mainly composed by soil carbon (Hadi et al. 2000). Hence it can be assumed as a microwave absorber. Based on the ground data, a model of scattered waves from burnt coal seam is considered, and assumed as figure 4.4. Figure 4.4 (a) shows the two-dimensional model of analysis composed of three media; infinite length of air, thickness ξ of burnt coal seam, and infinite depth of peat. In this research, the author is *not* considering the roughness of scattered surfaces. The incident wave is supposed to be a plane wave that has transverse electric (TE) mode with incident angle q_i. The equivalent circuit of this analysis model is shown in figure 4.4 (b), where effective impedance of burnt coal seam including impedance of burnt tree stand, impedance of peat, and input impedance are Z_C, Z_L, and Z_{TE}, respectively. In this analysis, peat is assumed to be an infinitely deep perfect conductor, because the water content is high. Consequently, Z_L is zero. Based on the transmission line theory (Gotoh *et.al* 2000, Robert 1992), the input impedance Z_{TE} is determined by

$$Z_{TE} = Z_C \frac{Z_L + Z_C \tanh g_C x}{Z_C + Z_L \tanh g_C x} \qquad (4.1)$$

where g_C and x are propagation constant and the thickness of burnt coal seam, respectively. Figure 4.5 shows propagation of TE wave that transmits from free space to burnt coal seam. Referring to this figure, the propagation constant g_C is derived from Maxwell's equations and obtained as;

$$g_c = j\frac{2p}{l}\sqrt{e_r m_r}\cos q_t \qquad (4.2)$$

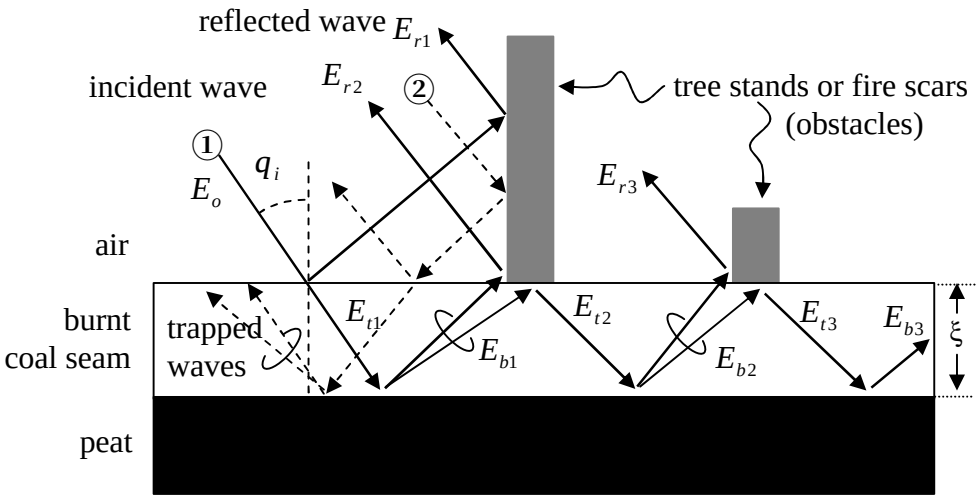

(a) Analysis model. Remarks: ① : burnt coal seam-obstacles scattering;
② : obstacles – burnt coal seam scattering

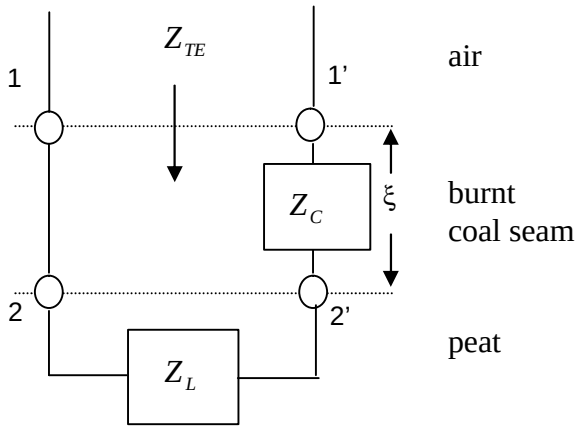

(b) equivalent circuit

Figure 4.4. Geometry of analysis

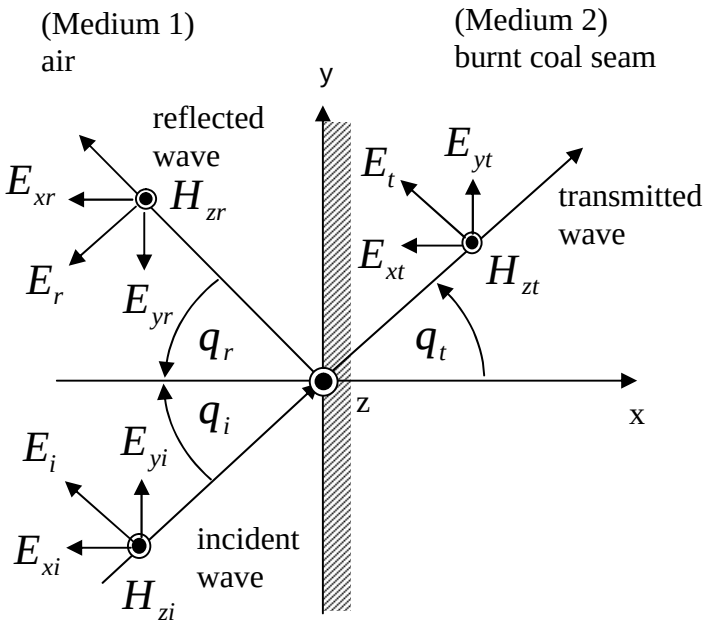

Figure 4.5. Geometry of wave propagation in two media.

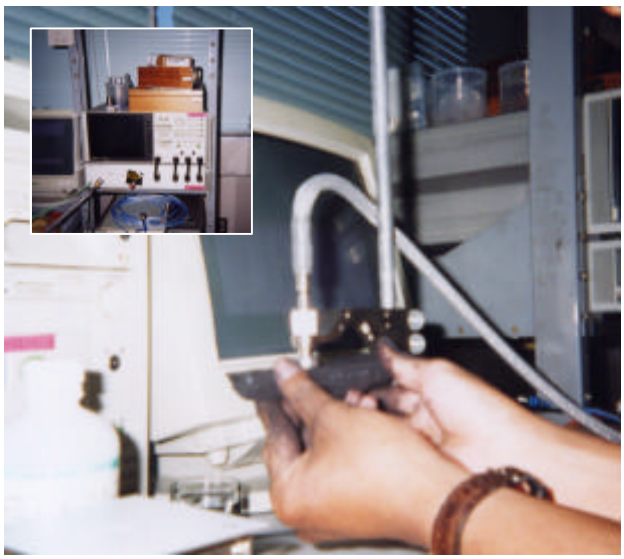

Figure 4.6. Measurement of burnt coal seam sample using dielectric constant kit HP85070B (see sub-figure)

where e_r, m_r, q_t, and l are complex dielectric constant, complex specific permeability, transmitted angle, and wavelength, respectively. The wave impedance of transmitted wave in burnt coal seam is obtained from component of electromagnetic fields that perpendicularly to the propagated axis (x-axis).

$$Z_C = E_{yt} / H_{zt} = Z_0 \sqrt{m_r / e_r} \cos q_t \tag{4.3}$$

where $Z_0 (= \sqrt{m_0 / e_0})$ is wave impedance in free space (=120p Ohms). Based on Snell's law, the relationship between incident angle q_i and transmitted angle q_t yields

$$\sin q_i / \sin q_t = \sqrt{e_r m_r} \tag{4.4}$$

Substituting (4.2) to (4.4) into (4.1), wave impedance Z_{TE} of input TE wave in burnt coal seam is

$$Z_{TE} = \frac{Z_0}{e_r} \sqrt{e_r m_r - \sin^2 q_i} \tanh\left(j \frac{2px}{l} \sqrt{e_r m_r - \sin^2 q_i} \right) \tag{4.5}$$

Further, the reflection coefficient is denoted by

$$\Gamma = \frac{Z_{TE} - Z_0 \cos q_i}{Z_{TE} + Z_0 \cos q_i} \tag{4.6}$$

Finally, by considering the far zone fields, the backscattering coefficient s^0 is derived as

$$s^0 = \frac{4pR^2}{A_o} \left\langle \left| \Gamma \frac{e^{-jkR}}{R} \right|^2 \right\rangle \tag{4.7}$$

where R is distance from targeted area to receiver or JERS-1 SAR sensor (antenna). R is distance from centre of tree trunk to sensor, $R = R' / \sin q_{is}$. Where R' is distance from trunk to sensor in range (horizontal) direction (refer figure 1.5). q_{is} is the incident angle of satellite illumination (JERS-1 SAR, $q_{is} = 38.7^o$). A_o is targeted surface area.

4.3 Simulation

In this study, the author simulates the scattered waves from burnt coal seam to explore the relationship between backscattering coefficient s^{o} and thickness x of burnt coal seam using Finite Difference Time Domain (FDTD) method (Yee 1966) and Mur method as absorbing boundary condition or external boundary condition (Mur 1981). The scattered fields were described by the same equations that were derived in Chapter II and III, and its derivation is discussed in Appendix C in detail.

Finally, the backscattering coefficient s^{o} was defined by (4.8), where E_y^I is observed electric field intensity in frequency $f = 1.275$ GHz of scattered wave that is scattered by only peat (perfect conductor).

$$s^{0} = \frac{4pR^2}{A_o}\left(\frac{\left\langle \left|E_z^S\right|^2 \right\rangle}{\left\langle \left|E_z^I\right|^2 \right\rangle}\right)_{f=1.275GHz} \tag{4.8}$$

Where E_z^S is far zone scattered field intensity that is observed by JERS-1 SAR sensor, $E_z^s = E_z^{scat}\, e^{-jkR}/R$. R is distance from centre of satellite illuminates area to JERS-1 SAR sensor (antenna), $R = R'/\sin q_{is}$. Where R' is distance from targeted area to sensor in range (horizontal) direction (refer figure 1.5). q_{is} is the incident angle of satellite illumination (JERS-1 SAR, $q_{is} = 38.7^{o}$). By substituting these relationships to (4.8), in this case, backscattering coefficient equation is not depending to distance R. A_o is area of scattered surface.

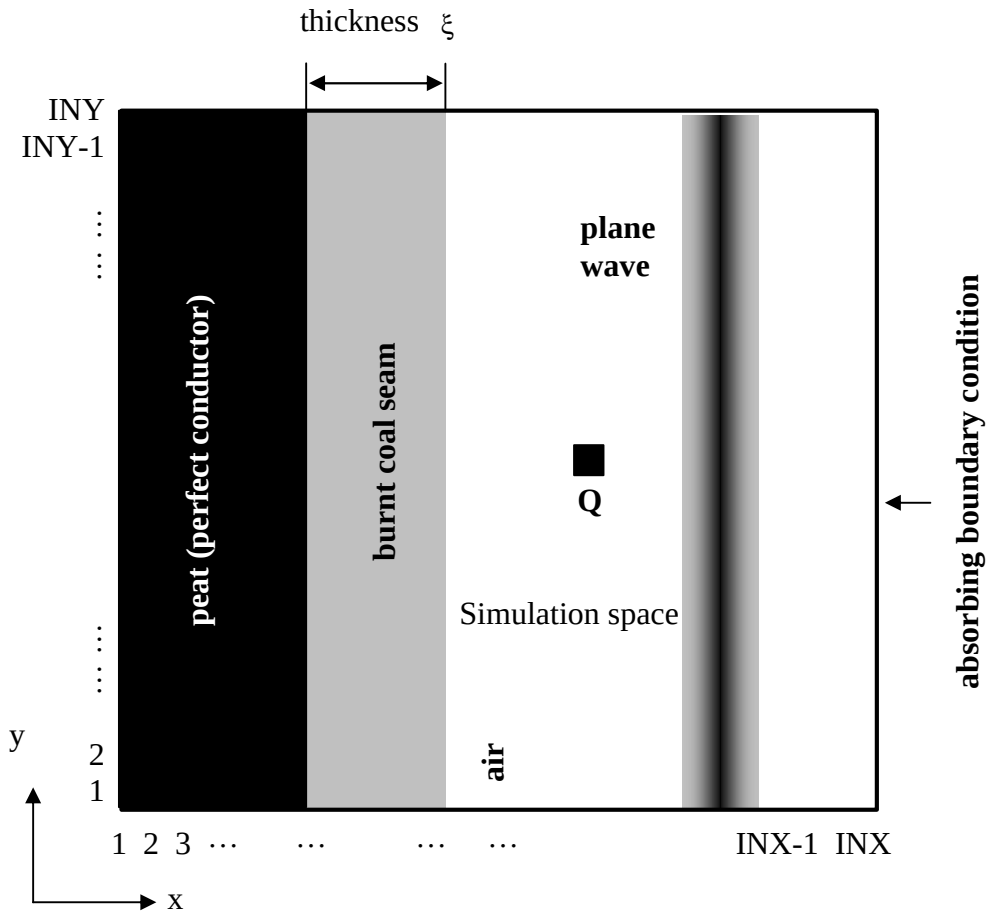

Figure 4.7. Simulation model.

4.4 Results

To confirm the analysis result with simulation result, the author defines a simple method by calculating only the logarithm of reflection coefficient (in power) that is defined by $s = 20\log(|\Gamma|)$ (tetuko *et al.* 2001b). Γ is reflection coefficient (4.6), where the reflection coefficient of simulation result is defined by $\Gamma = |E_y^S| / |E_y^I|$. The parameters in confirmation of analysis result are wave impedance $Z_o = 120p$ Ohms, specific permeability $m_r = 1$, dielectric constant $e_1 = 2.5 - j0.1$, wavelength $l = 23.5$ cm, incident angle $q_i = 0^o$ (horizontal) are used, and the thickness ξ of burnt coal seam varies from 0 to 1m. By substituting these parameters into (4.5) and (4.6), the reflection coefficient with respect to each ξ is obtained. Furthermore, by substituting these reflection coefficients into $s = 20\log(|\Gamma|)$, the correlation between ξ and s is obtained. This result is illustrated in figure 4.10 (analysis). This figure shows that increment in the thickness of burnt coal seam is directly proportional to reduction of s. It implies that the burnt coal seam absorbs wave energy.

Figure 4.7 shows the geometry of simulation space. The simulation is computed on 300 x 300 grids, where the time step is chosen as $\Delta t = 2.5\times10^{-11}$ s and a grid spacing of $\Delta x = \Delta y = 1.25\times10^{-2}$ m that fulfils the Courant conditions, running time $t = 600\Delta t$ s, dielectric constant e_0 and permeability m_0 of vacuum space are 8.854×10^{-12} F/m and $4p\times10^{-7}$ H/m, respectively. The initial place of incident pulse head *d* is located –150 grids from peat surface, and the maximum intensity of electric field E_o of Gaussian pulse is 1 V/m. Peat is defined as perfect conductor 0.5m deep that is equivalent to 40 grids. The thickness ξ is varied from 0m to 1m (0 to 80 grids). In figure 4.8, the scattered waves due to Gaussian

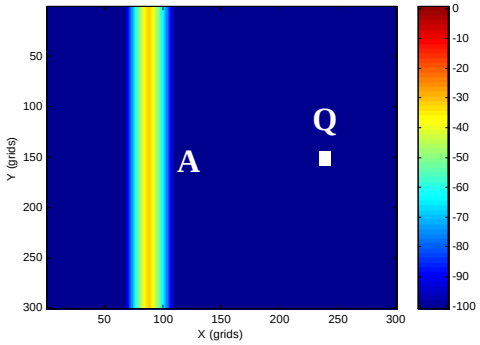

(a) $t = 150\Delta t$ s

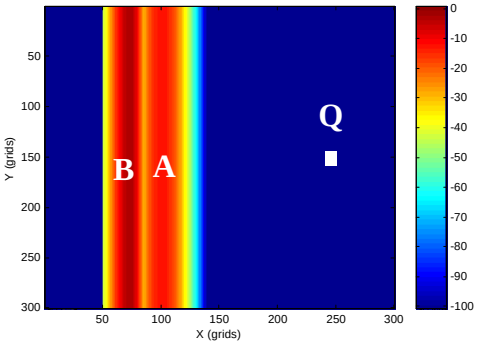

(b) $t = 200\Delta t$ s

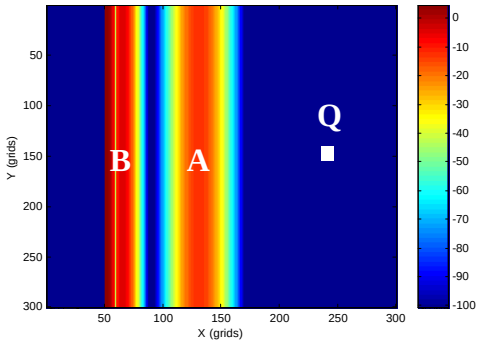

(c) $t = 250\Delta t$ s

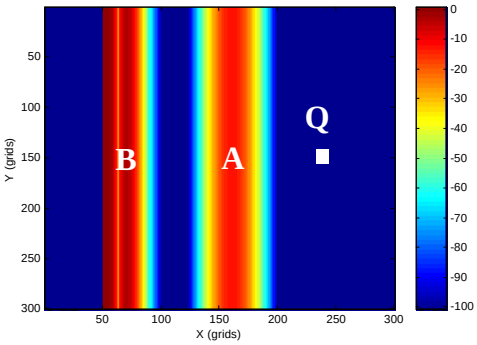

(d) $t = 300\Delta t$ s

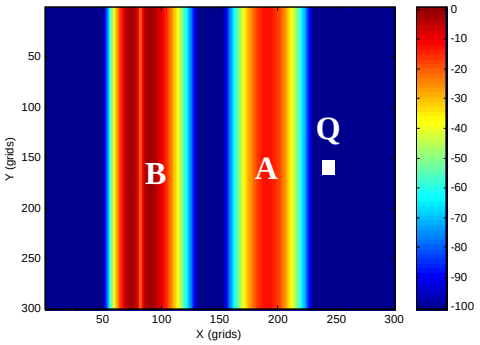

(e) $t = 350\Delta t$ s

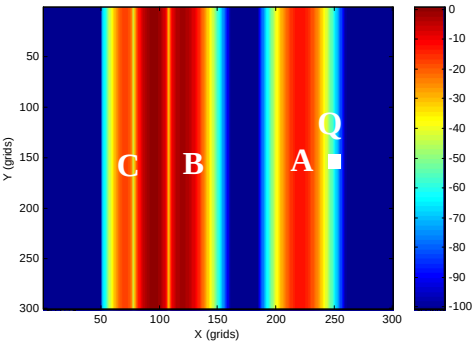

(f) $t = 400\Delta t$ s

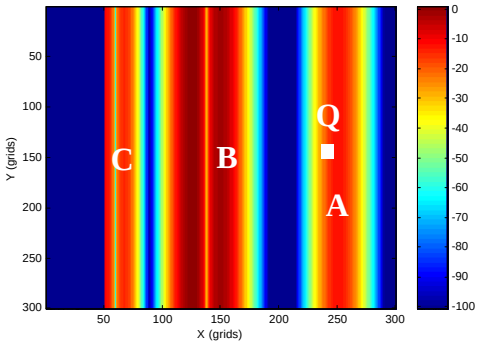

(g) $t = 450\Delta t$ s

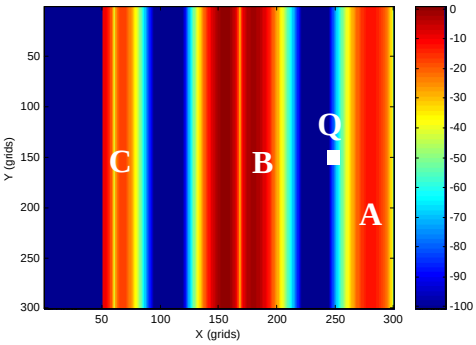

(h) $t = 500\Delta t$ s

Figure 4.8. Scattered waves in simulation space.

pulse of incident wave are shown. This shows only the scattered wave, because this study wants to solve the scattering problem. Scattered waves from burnt coal seam surface and peat surface are seen to propagate in running time $t = 0$ to $500\Delta t$ s and the thickness ξ is 0.5m. In this figure, A, B, and C show scattered waves from burnt coal seam surface, first and second waves reflected from peat surface, respectively.

Figure 4.9 shows the intensity of electric field E_y^S and magnetic field H_z^S observed at point Q with incident angle of incident pulse $f_0 = 0^o$. At this angle, the intensities of E_x^S are observed zero, because this component parallels to the direction of wave propagation. A and B are scattered waves from burnt coal seam surface and peat surface, respectively. The scattered waves A is attenuated until with –12.5 dB. Wave B has two maximum values or saddles, because it is reflected from peat surface or perfect conductor, so it means the differential of the incident pulse or Gaussian pulse. Additionally, wave B is wider than the incident wave. This is caused by the incident wave phase velocity being reduced by burnt coal seam when it is propagating through the medium. The frequencies spectrum of the observed scattered waves is obtained by its fast Fourier transformed. Then, we acquire the electric field intensity E_y^S of the JERS-1 SAR at frequency ($f = 1.275$ GHz). By considering the $s = 20\log(|\Gamma|)$, where $\Gamma = |E_y^S| / |E_y^I|$, s with respect to the thickness x are obtained and, together with the previous analysis result, is shown in figure 4.10. This figure shows that both results are in good agreement.

Finally, by considering multi-scattering (① and ② - wave propagation paths in figure 4.4 (a)) and the incident wave of satellite illumination (JERS-1 SAR, $q_{is} = 38.7^o$), the relationship between the two dimensional far zone backscattering coefficient and thickness of burnt coal seam is obtained and shown in figure 4.10 (JERS-1 SAR (far zone)). In next

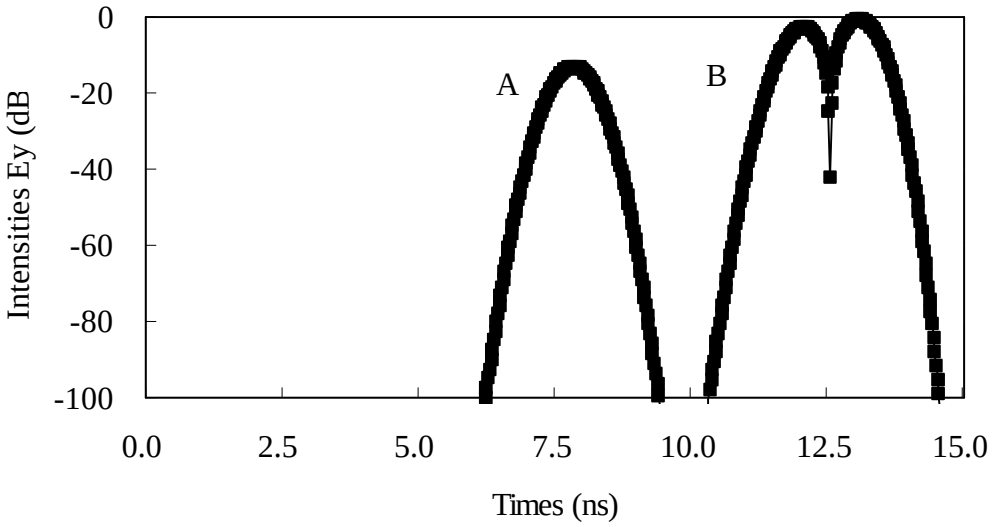

(a) Electric field E_y^S

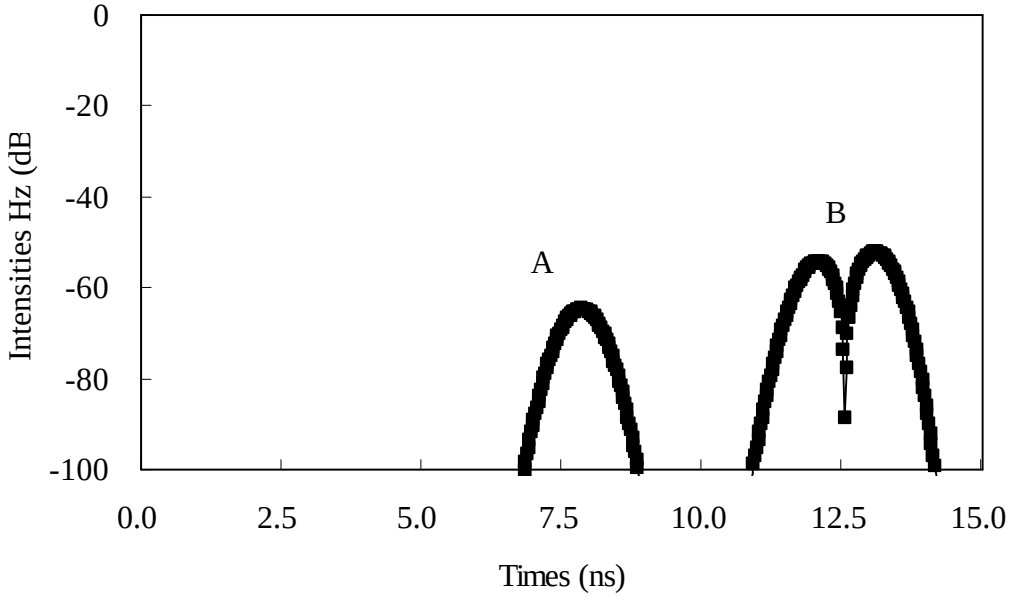

(b) Magnetic field H_z^S

Figure 4.9. Intensity of scattered wave in observed point Q.

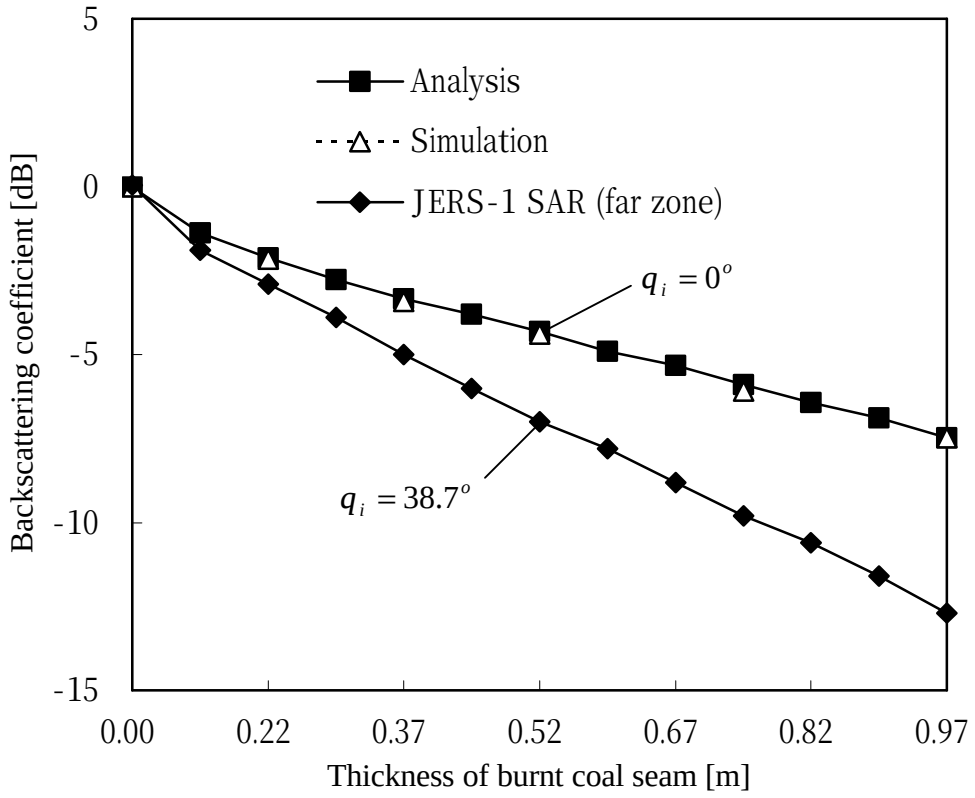

Figure 4.10. Relationship between burnt coal seam thickness and backscattering coefficient in two dimensional analysis and simulation.

section, the results are applied to estimate the thickness x of burnt coal seam in the study area.

4.5 Application

4.5.1 Study Area

The study area is located at 114°23′–114°45′E, 2°23′–2°47′S or at district of south Barito and Kapuas, central Borneo, Indonesia. The altitude of this area is ranging from 9m to 14m above sea level. The Barito and the Kapuas rivers encircle this area, and vegetation type of this area is tropical forest. This area is mainly covered by peat (soil with 40% to 60% coal content) and peat swamp (peat area with high water content). The climate on Borneo is wet all through the year with an average annual rainfall of around 3500mm to 4500mm, while the relative humidity varies between 70% and 90%.

Figure 4.1 shows photographs of the study area. Photographs A and B show the main types of vegetation namely tengkawang (*Dipterocarpus spp*), *pule* tree, and *purun* grass, that are found around the *Purun* river (black water river) in the study area. Photograph C shows burnt tengkawang and pule tree near the Bunter lake. Photograph D shows staffs boring peat to measure coal seam thickness. This ground survey was done during the period 1995 to 1997 in 'One Million Hectares Peatland Project' and photographs of its area are illustrated in Appendix D. The measurement results were mapped (DEPHUTBUN 1999, CSAR 1997) (figure 4.2). The detail ground data are shown in Appendix D.

Figure 4.11 (a) to (c) show geometric corrected raw data of JERS-1 SAR data that acquired on 15 May 1996 (before forest fires), 3 February 1997 (start forest fire), and 29 July 1997 (post forest fires). The composite data of these data is shown in figure 4.12, where 15 May 1996: blue, 3 February 1997: green, and 29 July 1997: red. This figure shows clearly that the opening area by burning forest is shown in red colour. By comparing visually with SPOT-HRV data that were acquired in closed date with these data (see figure 4.3 (a) to (d)), the red

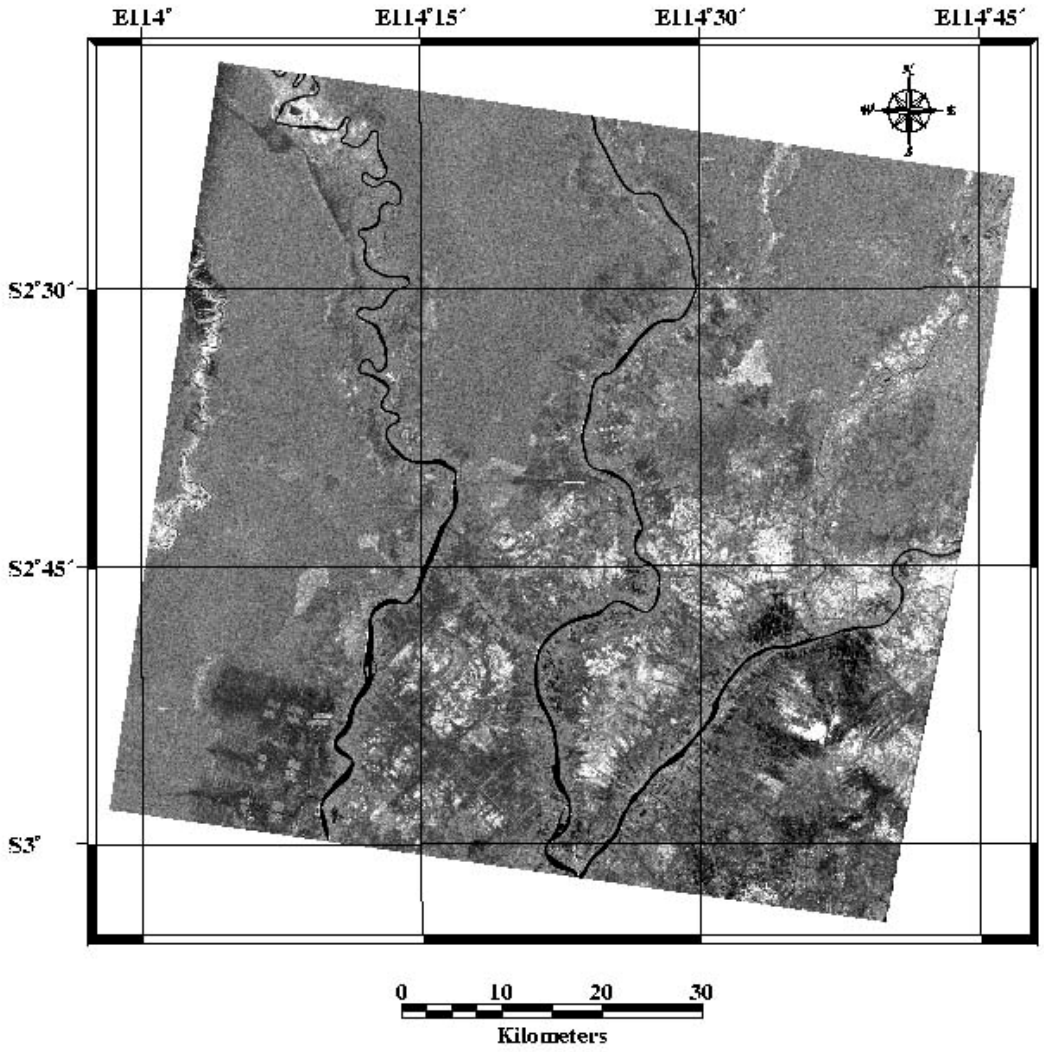

Figure 4.11. (a) Raw data of JERS-1 SAR: 15 May 1996

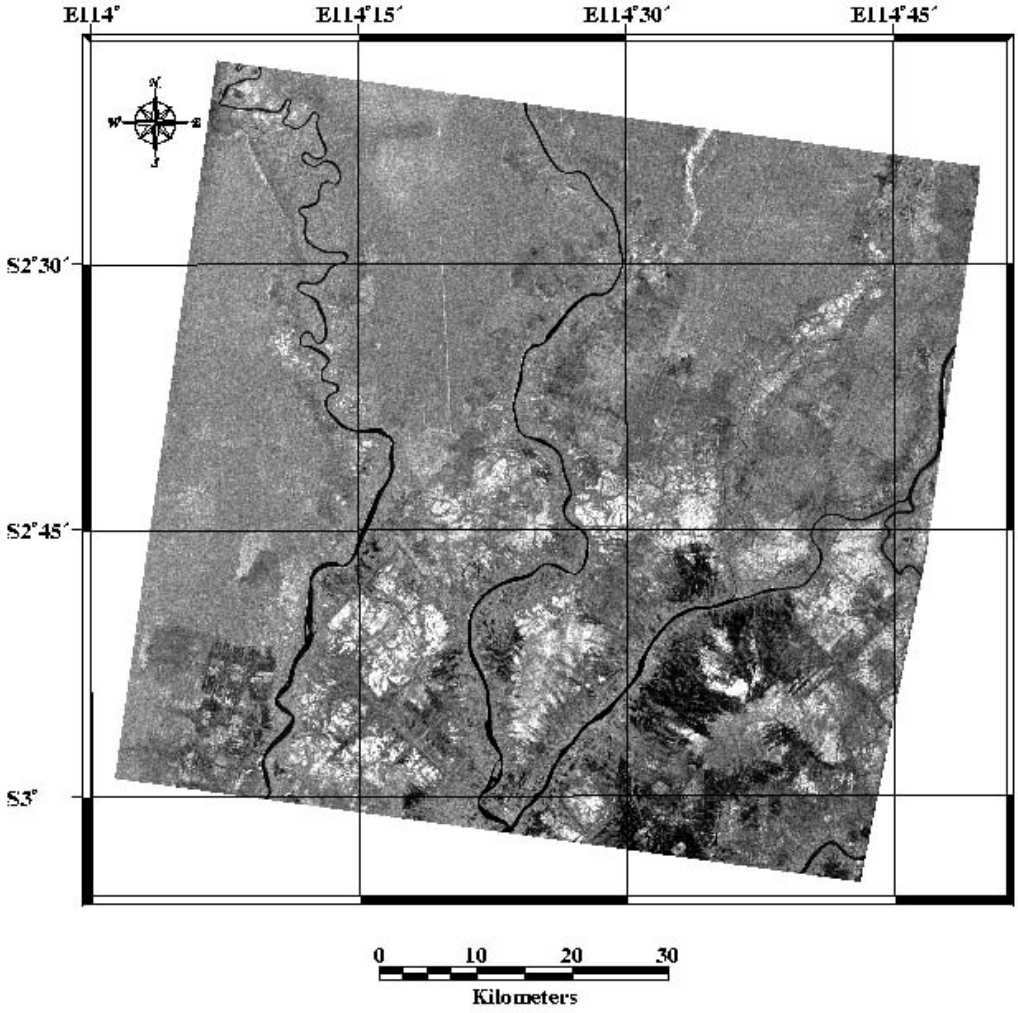

Figure 4.11. (b) Raw data of JERS-1 SAR: 3 February 1997

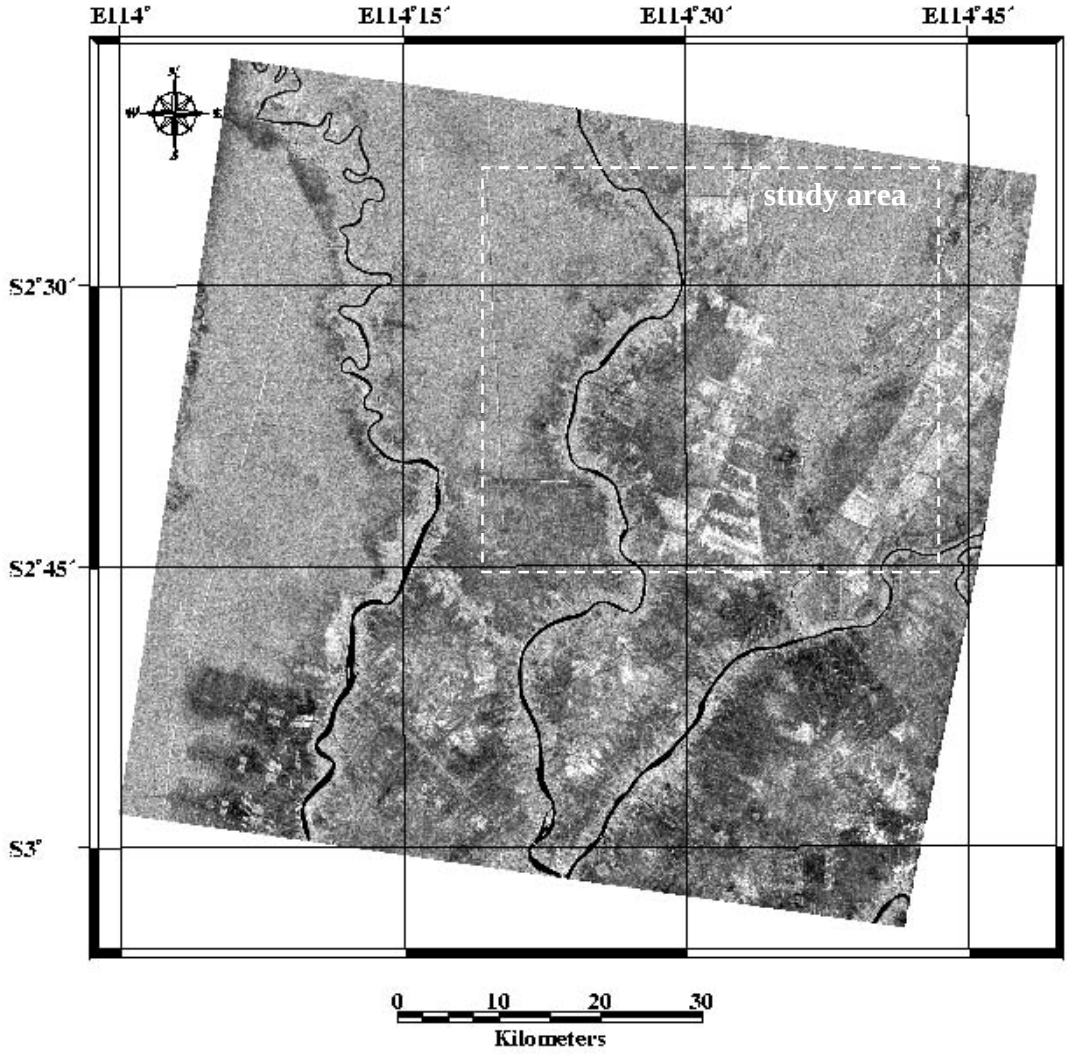

Figure 4.11. (c) Raw data of JERS-1 SAR: 29 July 1997: dotted line is the study area in this study

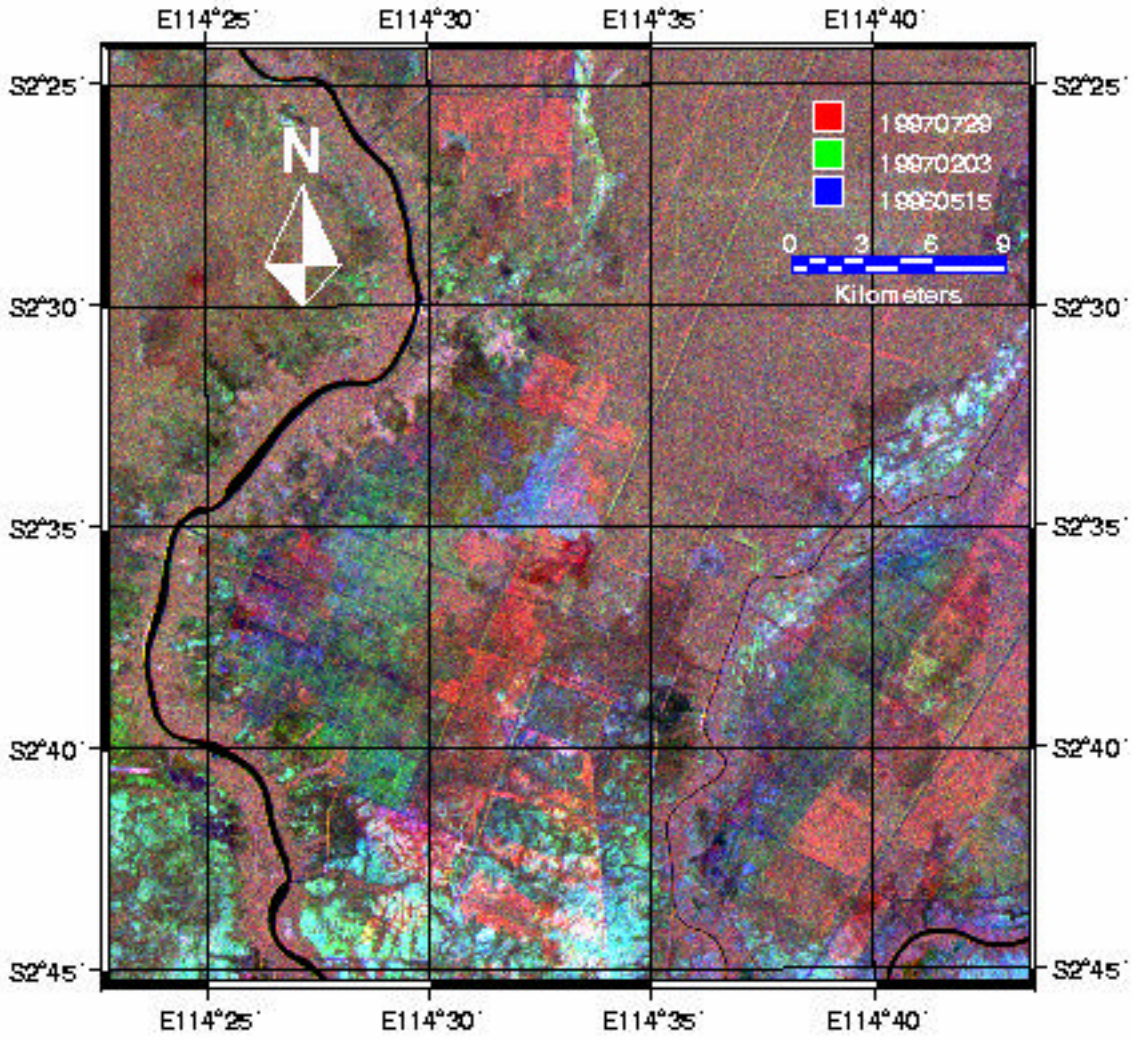

Figure 4.12. Composite of JERS-1 SAR data: red – 29 July 1997, green – 3 February 1997, blue – 15 May 1996

colour region shows that the huge forest fires were happened on 29 July 1997 and 7 August 1997. In this study, therefore, SAR data that acquired on 29 July 1997 is used to estimate the thickness of burnt coal seam in central Borneo area. The pre-processing of this data is explained in the next section.

4.5.2 Data Processing

The JERS-1 SAR data (path 95, row 305) that was acquired on 29 July 1997 (dry season and during fire events) is used to estimate the thickness of forest fire scars (burnt coal seam) in the study area. This data was processed at level 2.1 or standard geocoded data and was modified into Universal Transverse Mercator (UTM) projection by the Earth Observation Research Centre (EORC) of Japan National Space Development Agency (NASDA). First, a 3x3 median filter was employed and the second process used a 5x5 average filter to reduce inherent speckle noise (Sunar *et al.* 1998). At the same time, the data was also referenced to the UTM co-ordinate system, through a polynomial rectification using 30 ground control points collected from aerial (Bakosurtanal 1990) and topographic maps (Bakosurtanal 1991) of scale 1:50,000. This procedure yielded a geometric accuracy of 0.1pixels. Then the spatial resolution of SAR data was resampled to 12.5m.

A supervised classification was performed to classify the data. The study area was classified into six classes based on aerial and topographic maps and ground data as reference to collect six classes of the training sets. The classes were paddy field, bush swamp, forest, bush land, burnt coal seam, and settlement. In this research, the burnt coal seam class is considered in estimation of thickness ξ. Furthermore, SPOT HRV data (figure 4.3) were assessed to identify the fire spots in the study area. Then burnt coal seam was unsupervised-classified into four classes as shown in figure 4.13. The statistic value (average) of each class

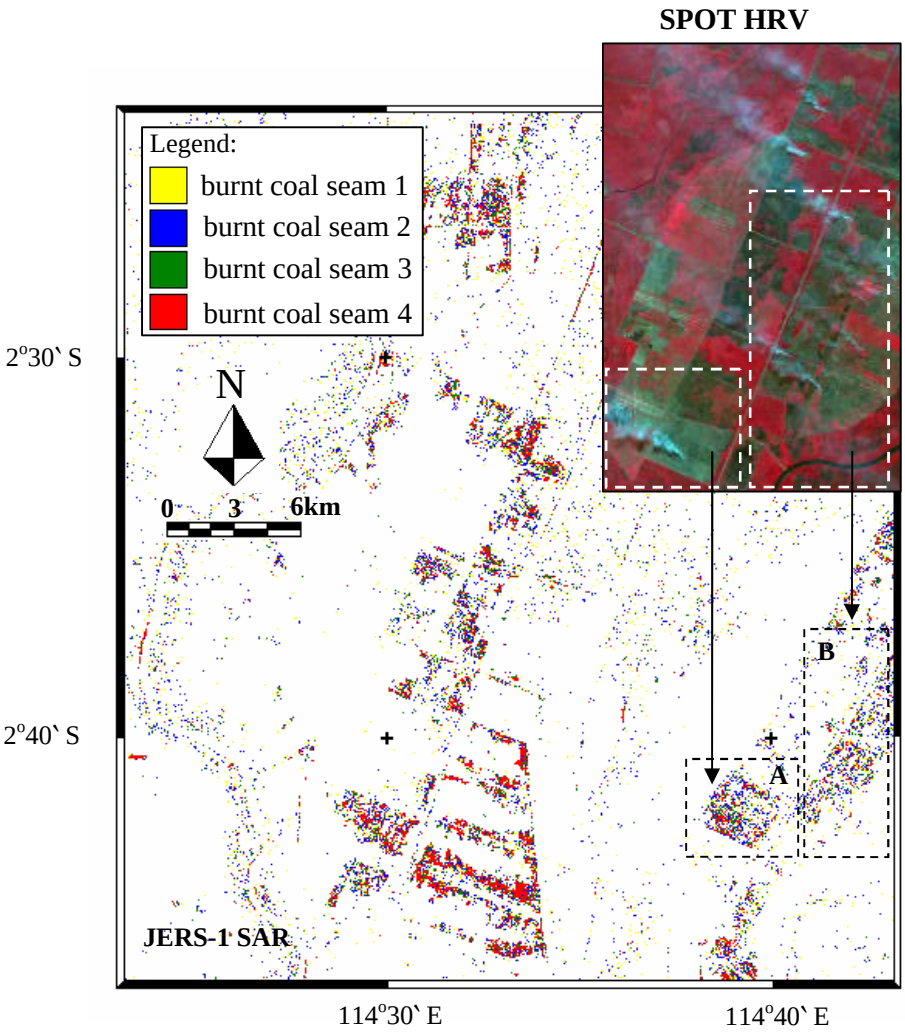

Figure 4.13. A SPOT-HRV data and supervised classification results of a JERS-1 SAR data (path 95, row 305, 27 July 1997).

Table 4.1. Thickness of burnt coal seam in the study area

Class names	Backscattering coefficient s^o (dB)	Burnt coal seam thickness ξ (m)	Standard deviation (m)
Burnt coal seam 1	-7.0	0.52	0
Burnt coal seam 2	-6.5	0.47	0.015
Burnt coal seam 3	-5.8	0.40	0.015
Burnt coal seam 4	-5.0	0.37	0.015

was obtained and the backscattering coefficients s^o are calculated using equation $s^o = 20\log I - 68.2\,\text{dB}$ (known as NASDA calibrated equation) (Shimada 1998). Where I is pixel intensity of JERS-1 SAR data. By comparing this with graph (JERS-1 SAR) in figure 4.10, ξ of each class was acquired (refer Table 4.1), where the thickness of burnt coal seam ξ in the study area are between 0.37m and 0.52m. This result was confirmed by ground data (figure 4.2 (b)), especially area A and B in figure 4.13, which matched the analysis. The result shows the fires reach 0.52 m in depth (thickness) of burnt coal seam.

4.6 Conclusions

Numerical analysis was conducted to analyse the relationship between the logarithm of reflection coefficient (in power) s and the burnt coal seam thickness ξ with incident angle $q_i = 0^o$. Then the analysis result was confirmed by simulation using Finite Difference Time Domain (FDTD) method. They are in good agreement. The relationship between backscattering coefficient s^o and the thickness of burnt coal seam ξ was obtained by considering the incident angle of Japanese Earth Resources Satellite (JERS-1) SAR with

incident angle $q_{is} = 38.7^{o}$. This result was applied successfully in estimating the burnt coal seam thickness in central Borneo, Indonesia. This result was confirmed by the ground data that was collected by ground survey done in 1995 to 1997, and it shows that fires could reach 0.52 m in depth (thickness). This was in good agreement with ground data. Further, application of this result can be used to estimate fire scars thickness, which is very important to extinguish forest fire effectively and accurately.

References

1. BAKOSURTANAL, 1990, Aerial map: Sungai Mantangai 1713-51. scale 1:50 000, National Coordination Agency for Surveys and Mapping, 1st edition (Cibinong: BAKOSURTANAL).
2. BAKOSURTANAL, 1991, Topographic maps: Rimbun Tulang 1713-24, Jenamas 1713-52, Dadahup 1713-23. scale 1:50 000, National Coordination Agency for Surveys and Mapping, 1st edition (Cibinong: BAKOSURTANAL).
3. BURHANUDDIN SARBINI, 2000, Report of Peatland Project, Indonesian Ministry of Forestry and Estate Crops Meeting, 9 March 2000 (Jakarta: Planological Agency)
4. CSAR, 1997, Coal seam thickness map: one million hectares peatland project: PLG-A. scale 1:50 000, Centre for Soil and Agroclimate Research, 1st edition (Bogor: CSAR).
5. DEPHUTBUN, 1999, One Million Hectare Peatland Project, Indonesian Ministry of Forest and Estate (Jakarta: DEPHUTBUN)
6. DAVID, P., STELLA, E.B., STHEPHEN, J.M., 1997, Terrain influences on SAR backscatter around mt. Taranaki, New Zealand. IEEE Transactions on Geoscience and Remote Sensing, 35, 924-932.
7. GOTOH K., YAMAZAKI J., 2000, Electromagnetics Problems Solving, 122nd edition (Tokyo: Kyoritsu).
8. HADI, A., 1999, Lambung Mangkurat University, Borneo, Indonesia (private communications).
9. HADI, A., INUBUSHI, K., RAZIE, F., PURNOMO, E., YUSRAN, F. H., and TSURUTA, H., 2000, Dynamics of methane and nitrous oxide in the tropical peats. The impacts of land-use/cover change on greenhouse gas emissions in tropical asia, edited by Murdiyarso, D. and Tsuruta, H., 1st edition (Bogor: IC-SEA NIAES), pp.35-51.

10. KASDI, S., 1999, Centre for Soil and Agroclimate Research, Indonesia (private communications).
11. MUR, G., 1981, Absorbing boundary Conditions for the finite-difference approximation of the time-domain electromagnetic-field equation. IEEE Transactions on Electromagnetic Compatibility, 23,377-382.
12. ROBERT E. COLLIN, 1992, Foundations for Microwave Engineering. 20th edition (Singapore: McGraw Hill).
13. SHIMADA, M., 1998, User's guide to NASDA's SAR products. Earth Observation Research Centre (EORC), National Space Development Agency (NASDA), 2nd edition (Tokyo: EORC-NASDA).
14. SUNAR, F., TABERNER, M., MAKTAV, D., KAYA, S., MUSAOGLU, N., YAGIZ, E., 1998, The use of multitemporal radar data in agriculture monitoring: a case study in Kyocegiz-Dalaman ecosystem, Turkey. International Archives of Photogrammetry and Remote Sensing, 32, 559-565.
15. TETUKO S.S., J., TATEISHI, R., WIKANTIKA, K., 2001a, A method to estimate tree trunk diameter and its application to discriminate Java-Indonesia tropical forest. International Journal of Remote Sensing, 22, 177-183.
16. TETUKO S. S., J., TATEISHI, R., TAKEUCHI, N., 2001b, Estimation of burnt coal seam thickness in central Borneo using a JERS-1 SAR data. International Journal of Remote Sensing (in press).
17. UNO TORU, 1998, Finite Difference Time Domain Method for Electromagnetic Field and Antenna Analyses. 1st edition (Tokyo: Corona).
18. YEE, K.S., 1966, Numerical solution of initial boundary value problems involving Maxwell's equations in isotropic media. IEEE Transactions on Antennas Propagation,14, 302-307.